A Systematic State–Space Approach to Large-Signal Transistor Modeling

Matthias Seelmann-Eggebert, Thomas Merkle, Friedbert van Raay, Rüdiger Quay, *Member, IEEE*, and Michael Schlechtweg

***Abstract*—A state–space approach to large-signal (LS) modeling of high-speed transistors is presented and used as a general framework for various model descriptions of the dispersive features frequently observed for HEMTs at low frequency. Ensuring unrestricted LS–small-signal (SS) model compatibility, the approach allows to construct LS models from multibias SS S-parameter measurements. A general transformation between state–space models is derived, which are equivalent in the SS limit, but nonequivalent under LS stimuli. This transformation has the potential to compensate deviations observed by comparing model predictions with LS measurements and to find an optimum state linear LS model without any change of the SS behavior.**

***Index Terms*—GaN HEMT, large-signal (LS) transistor modeling, low-frequency (LF) dispersion, state–space approach.**

I. Introduction

LARGE-SIGNAL (LS) compact modeling of HEMTs has been a field of high research activity for over two decades. An LS model has to reproduce the complex dynamic of the transistor, which results from the subtle interplay of nonlinearity and memory effects. In the frequency domain, memory effects manifest themselves as dispersion, i.e., as a frequency dependence of the transfer function of the transistor two-port. To be positioned between the physics-based [1], [2] and black box [3], [4] approaches, physics-oriented semiempirical models are compact and enable efficient simulation. A variety of approaches can be found in the literature [5], [6] (and references therein), which differ by model topology and parameterization of the descriptive functions. For transistors not yet developed to perfection such as GaN HEMTs, the accuracy of semiempirical models often limits the overall reliability of nonlinear circuit simulation or is bounded to a bias region. The objective of this paper is to relate compact transistor modeling with the concepts of linear control theory [7] and, by an natural extension to nonlinear dispersion effects, exploit these in view of possible model improvements.

II. Compact HEMT Modeling

Most compact LS models build the transistor from a nonlinear intrinsic part by embedding it into a linear parasitic network. The intrinsic part contributes nonlinear resistive and displacement currents. In the simplest picture, these currents are attributed to drain and gate current sources and gate charges, which are immediate functions of intrinsic voltages and, hence, independent of the system history [6], [8].

In a more realistic physical picture, both fixed and free charge carriers, which contribute to the terminal currents, result from a complex (and strongly bias dependent) interaction of transport, generation, and recombination processes, and a simple description by voltage-controlled charge and current sources cannot completely account for the frequency dependence of the device response. Therefore, it is common practice to add delay mechanisms for charge [9], current [10], or voltage [11] in order to model magnitude and phase of all four S-parameters correctly. Nevertheless, the concept that the intrinsic charge and current sources are immediate functions of two intrinsic voltages is retained. If the existence of such state functions is taken for granted, then there result integrability conditions, which impose restrictions on the small-signal (SS) parameters [8]. A general compatibility of the small-signal equivalent (SSE) circuit and the LS model is not achieved anymore [11]. For GaN HEMTs, the integrability conditions are no longer satisfied on a global scale. Hence, current and charge functions give only an approximative reproduction of the S-parameters, and the degree of deviation depends on the bias.

Furthermore, HEMT devices often show the behavior that their dc characteristics differ from the resistive current state function obtained by integration of the S-parameters at high frequencies (HFs) in the gigahertz range. In the Root model [12, p. 289], the existence of an additional state function is postulated to describe the HF current. The transition from this HF current state function to the dc characteristics is accomplished via a low-pass function. The dc-HF deviation is attributed to the influence of fixed charges [13], which modify the electric field and, as a consequence, affect the control voltages. Being influenced by the bias, these charges are thought to be trapped by imperfections located either at the surfaces between the electrodes or the substrate buffer adjacent to the channel [14]. Since their capture time constants are in the order of some microseconds, the traps cause dispersive features at frequencies below 10 MHz [low-frequency dispersion (LFD)]. However, S-parameter systems for characterization of HF transistors have a low-frequency (LF) limit of typical 45 MHz, where the LFD features are absent. As a further LFD mechanism for power devices, we have to consider self-heating and the related thermal memory effects [12]. Parker and Rathmell [15] have illustrated a description of LFD by three state variables, which are determined by first-order differential equations.

Manuscript received May 18, 2006; revised October 2, 2006. This work was supported by the Federal Ministry of Defense (BMVg) and by the Federal Ministry of Education and Research (BMBF).

M. Seelmann-Eggebert, F. van Raay, R. Quay, and M. Schlechtweg are with the Fraunhofer Institute of Applied Solid State Physics, D-79108 Freiburg, Germany (e-mail: seelmann@iaf.fraunhofer.de).

T. Merkle is with the CSIRO ICT Centre, Epping, N.S.W. 1710, Australia (e-mail: thomas.merkle@csiro.au).

Color versions of one or more of the figures in this paper are available online at http://ieeexplore.ieee.org.

Digital Object Identifier 10.1109/TMTT.2006.889154

An LS model is frequently constructed from multibias SS S-parameter data taken over a wide range of frequencies. For model construction, the S-parameter data set has to be complete, i.e., S-parameter have to be measured on a narrow voltage grid covering the complete accessible bias range or at least a large region of interest (ROI). Throughout this paper, two different models, which reproduce the same complete S-parameter data set and the dc characteristics, are said to have the same SS signature. Often a model is verified by comparison of its predictions with LS load–pull and power-sweep measurements. In the semiempirical model approaches, the SS signature leads to a unique model since the state functions are completely determined by path integration of the SS parameters. Hence, there remain no degrees of freedom for fine tuning the LS behavior of the model and a tradeoff between the match of the LS data and the global match of the SS data may have to be met. However, this predictive dependence of LS data on SS data is a consequence of the chosen state representation and is relaxed for models containing more or different state variables.

The goal of this paper is to tie together the semiempirical modeling approach for transistors, particularly HEMTs, and the state–space approach for modeling dynamic systems. In electronics, the state–space approach has been used since the 1960s [16], when it was applied to network analysis. Recently, the state–space approach was discussed for artificial neural network (ANN) modeling of nonlinear microwave circuits [4]. A modified state–space approach to behavioral circuit modeling was introduced by Root *et al.* [17].

In Section III, a general scheme for state–space modeling of transistors is presented. In Section IV, we will develop a general method of constructing a pool of LS models from a complete set of S-parameters. In Section V, the proposed model construction method is applied to the standard SS field-effect transistor (FET) equivalent circuit. In Section VI, various one- and two-mode model approaches for LFD are discussed and compared with experimental power-sweep data for a GaN transistor.

III. Nonlinear State Variable Approach

A. Systems Equations and State Functions

We consider a system with the input variables $\mathbf{u} = (u_1, \ldots, u_{nI})$ and the output variables $\mathbf{i} = (i_1, \ldots, i_{nO})$. For the transistor two-port ($n_I = n_O = n_{io} = 2$), we may choose the port voltages $\mathbf{u} = (u_{\mathrm{GS}}, u_{\mathrm{DS}})$ as the input vector and the respective currents $\mathbf{i} = (i_G, i_D)$ as the output vector. In addition, the system has internal degrees of freedom ("states" or "modes"). At a given time, the system resides at a distinct system state, characterized by the state variable vector $\boldsymbol{\theta} = (\theta_1, \ldots, \theta_{\mathrm{ns}})$. The number of independent state variables n_S is called the *order of the system*. In generalization of the linear approach [7], the state variable vector $\boldsymbol{\theta}$ evolves driven by a first-order differential equation

$$\frac{d}{dt}\boldsymbol{\theta} = \mathbf{F}^{\boldsymbol{\theta}}(\boldsymbol{\theta}, \boldsymbol{u}). \tag{1}$$

The state equation (1) is the basis for nonlinear systems theory and bears a rich variety of phenomena such as limit cycles, erratic, or even chaotic behavior [18]. The output vector $\mathbf{i}$ depends not only on the system input, but also on the system state, as described by the output equation

$$\mathbf{i} = \mathbf{G}^{\boldsymbol{I}}(\boldsymbol{\theta}, \mathbf{u}). \tag{2}$$

In the canonical form (1) and (2), the functions $\mathbf{F}^{\theta}$ and $\mathbf{G}^{I}$ depend neither on the output entities, nor on the derivatives of the input entities. A complete description of the system requires knowledge of the system state function $\mathbf{F}^{\theta}$ and output state function $\mathbf{G}^{I}$. A system description by the canonical form (1) and (2) is called a state–space model [18] or macro model [19]. It bears a huge amount of information, which in numerical form has to be provided by $n_s + n_{io}$ function tables in $n_s + n_{io}$ dimensions. A state–space model can be directly implemented in commercially available nonlinear circuit simulators. For any given waveform $\mathbf{u}(t)$ of the system stimulus, the state equations are solved in the time domain in a straightforward manner [7] to obtain the output response $\mathbf{i}(t)$. In the frequency domain, (1) can be solved in an iterative manner by harmonic-balance algorithms. The state equation system is capable to model nonlinear systems in depth, in particular, combined effects of nonlinearity, short-term, and long-term memory.

Under equilibrium conditions, we solve (1) to obtain the equilibrium state function

$$\boldsymbol{\theta} = \boldsymbol{\theta}^{\mathrm{DC}}(\mathbf{u}) \tag{3}$$

which, by definition, satisfies

$$\mathbf{F}^{\theta}(\boldsymbol{\theta}^{\mathrm{DC}}(\mathbf{u}), u) = 0. \tag{4}$$

For slight perturbations from equilibrium, a second-order Taylor expansion of the state function with respect to the state vector yields

$$\mathbf{F}^{\boldsymbol{\theta}}(\boldsymbol{\theta}, \boldsymbol{u}) = -\mathbf{Q}_R(\mathbf{u})(\boldsymbol{\theta} - \boldsymbol{\theta}^{\mathrm{DC}}(\mathbf{u})) + \mathbf{P}_C(\mathbf{u})(\boldsymbol{\theta} - \boldsymbol{\theta}^{\mathrm{DC}}(\mathbf{u})) \cdot(\boldsymbol{\theta} - \boldsymbol{\theta}^{\mathrm{DC}}(\mathbf{u})) + \mathbf{r}(\boldsymbol{\theta}, \mathbf{u}). \tag{5}$$

The $n_S \times n_S$-matrix $\mathbf{Q}_R$ of the linear term we call the relaxation matrix

$$(\mathbf{Q}_R(\mathbf{u}))_{ik} = -\frac{\partial}{\partial\theta_k} F_i^{\theta}(\boldsymbol{\theta}^{\mathrm{DC}}(\mathbf{u}), \mathbf{u}). \tag{6}$$

The $n_s \times n_s \times n_s$-tensor $\mathbf{P}_C$ of the quadratic term we call the relaxation curvature tensor

$$(\mathbf{P}_C(\mathbf{u}))_{nij} = \frac{1}{2}\frac{\partial^2}{\partial\theta_i\partial\theta_j} F_n^{\theta}(\boldsymbol{\theta}^{\mathrm{DC}}(\mathbf{u}), \mathbf{u}). \tag{7}$$

According to (4), the zeroth-order term in (5) vanishes and the residual term $\mathbf{r}(\boldsymbol{\theta}, \mathbf{u})$ is of third order in $\boldsymbol{\theta}$.

In the following, we assume that there exists an eigenvalue decomposition of the relaxation matrices, and all eigenvalues are nonzero. The delay matrix $\mathbf{T}_R(\mathbf{u}) = Q_R^{-1}(\mathbf{u})$ as the inverse of the relaxation matrix exists and can be written in terms of an

eigenvector matrix $\mathbf{A}_R(\mathbf{u})$ and a diagonal matrix $\boldsymbol{\tau}(\mathbf{u})$ with diagonal elements resembling the delay times of the system modes

$$\mathbf{T}_R(\mathbf{u}) = \mathbf{A}_{\boldsymbol{R}}(\mathbf{u})\boldsymbol{\tau}(\mathbf{u})\mathbf{A}_{\boldsymbol{R}}^{-\mathbf{1}}(\mathbf{u}). \tag{8}$$

Under equilibrium conditions, the output state function $\mathbf{G}^I(\boldsymbol{\theta}, \mathbf{u})$ yields

$$\mathbf{i} = \mathbf{i}^{\mathrm{DC}}(\mathbf{u}) = \mathbf{G}^I(\boldsymbol{\theta}^{\mathrm{DC}}(\mathbf{u}), \mathbf{u}). \tag{9}$$

For system states not too far from equilibrium, we obtain by Taylor expansion of (2) up to second order with respect to the state vector

$$\begin{aligned}\mathbf{i}(\boldsymbol{\theta}, \mathbf{u}) = \mathbf{i}^{\mathrm{DC}}(\mathbf{u}) + \boldsymbol{\Gamma}(\mathbf{u})(\boldsymbol{\theta} - \boldsymbol{\theta}^{\mathrm{DC}}(\mathbf{u})) \\ + \boldsymbol{\Xi}(\mathbf{u})(\boldsymbol{\theta} - \boldsymbol{\theta}^{\mathrm{DC}}(\mathbf{u}))(\boldsymbol{\theta} - \boldsymbol{\theta}^{\mathrm{DC}}(\mathbf{u})) + \mathbf{r}^{\mathbf{I}}(\boldsymbol{\theta}, \mathbf{u})\end{aligned} \tag{10}$$

where the output matrix $\boldsymbol{\Gamma}(\mathbf{u})$ and the output curvature tensor $\Xi(\mathbf{u})$ are defined by

$$(\boldsymbol{\Gamma}(\mathbf{u}))_{nm} = \frac{\partial}{\partial\theta_m} G_n^I(\boldsymbol{\theta}^{\mathrm{DC}}(\mathbf{u}), \mathbf{u}) \tag{11}$$

$$(\boldsymbol{\Xi}(\mathbf{u}))_{nij} = \frac{1}{2}\frac{\partial^2}{\partial\theta_i\partial\theta_j} G_n^I(\boldsymbol{\theta}^{\mathrm{DC}}(\mathbf{u}), \mathbf{u}). \tag{12}$$

The equilibrium output function $\mathbf{i}^{\mathrm{DC}}(\mathbf{u})$ describes the bias dependence of the output vector under equilibrium conditions. Please note that all matrices and tensors in (5)–(12), as well as the equilibrium state and output functions, are unique functions of the input vector $\mathbf{u}$ only. If the curvature term of the state function (5) or the output function (10) can be neglected, we say the system is relaxation state linear (RSL) or output state linear (OSL), respectively.

If we consider only system states close to equilibrium, we can truncate the Taylor series of *both* system functions (5) and (10) after the linear term and denote the system as state linearized. A state linear system obeys the simplified set of system equations

$$\boldsymbol{\theta} + \mathbf{T}_R(\mathbf{u})\frac{d}{dt}\boldsymbol{\theta} = \boldsymbol{\theta}^{\mathrm{DC}}(\mathbf{u}) \tag{13}$$

$$\mathbf{i} = \mathbf{i}^{\mathrm{DC}}(\mathbf{u}) + \boldsymbol{\Gamma}(\mathbf{u})(\boldsymbol{\theta} - \boldsymbol{\theta}^{\mathrm{DC}}(\mathbf{u})). \tag{14}$$

For the state linear relaxation equations (13), a time-domain solution is given by the series

$$\boldsymbol{\theta}(t) = \sum_{n=0}^{\infty}\left(-\mathbf{T}_R(\mathbf{u}(t))\frac{d}{dt}\right)^n \boldsymbol{\theta}^{\mathrm{DC}}(\mathbf{u}(t)). \tag{15}$$

For moderate variations with time, the output current shows a short time memory effect and the dc current is modified by a (generalized) displacement current obtained by truncating the series (15) after the second term

$$\begin{aligned}\mathbf{i} &= \mathbf{i}^{\mathrm{DC}}(\mathbf{u}) - \boldsymbol{\Gamma}(\mathbf{u})\mathbf{T}_R(\mathbf{u})\frac{d}{dt}\boldsymbol{\theta}^{\mathrm{DC}}(\mathbf{u}) + \cdots \\ &\approx \mathbf{i}^{\mathrm{DC}}(\mathbf{u}) + \mathbf{i}^{DP}(\mathbf{u}).\end{aligned} \tag{16}$$

Even for a state linear system, all state functions may depend on the input vector $\mathbf{u}$ in a highly nonlinear way. For frequency-domain-based simulators, RSL systems have the particular advantage that the state equations for a (periodic) time dependence of $\boldsymbol{\theta}^{\mathrm{DC}}(\mathbf{u}(\mathbf{t}))$ and $\mathbf{T}_R(\mathbf{u}(\mathbf{t}))$ can be solved in a single step. Hence, an RSL type of model facilitates direct extraction of parameters from LS measurements without involved harmonic-balance calculations.

B. Equivalent State Transformations

In the common situation, the state variables of the transistor are not directly measured, but are only indirectly observed by their effect on the output. This fact has the interesting implication that a state–space model is not unique, but there is always a number of exactly equivalent model representations and related state functions. Two representations are equivalent if any arbitrary stimulus of the two-port device produces identical voltage and current responses. The class of mutually equivalent model representations is characterized by the group of transformations under which the nonlinear system eqautions (1) and (2) are invariant. We consider an invertible otherwise arbitrary nonlinear state transformation

$$\boldsymbol{\theta}' = \mathbf{h}(\boldsymbol{\theta}). \tag{17}$$

Invariance means that the canonical form of the system equations, when expressed in terms of the transformed state variables, is retained as follows:

$$\frac{d}{dt}\boldsymbol{\theta}' = \mathbf{F}'^{\boldsymbol{\theta}}(\boldsymbol{\theta}', \mathbf{u}) \tag{18}$$

$$\mathbf{i} = \mathbf{G}'^{I}(\boldsymbol{\theta}', \mathbf{u}). \tag{19}$$

The new state functions and the associated functions of the state-linearized limit can be expressed by the original functions, the state transform, and its Jacobian matrix, as listed in Table I. The transformation rules for the system functions (Table I: R3 and R4) and the equilibrium state function (Table I: R5) are verified by inserting (17) into (1), (2), and (4). Taylor expansion of the new system functions according to (5) and (10) with respect to the new state variables about the transformed equilibrium state yields the transformation rules for the output and relaxation matrices. The new relaxation matrix is given by a similarity transform of the original one. Hence, the delay times are independent of the state representation. The equilibrium output function is also not affected.

The invariance of the system equations with respect to state transforms has the important consequence that no unique state functions $\mathbf{F}^{\theta}$ and $\mathbf{G}^I$ can be obtained by experiment unless the state variables $\boldsymbol{\theta}$ are accessible directly by independent measurement. In general, we have to exclude this option and rely solely on measurements of the system response $\mathbf{i}$. Hence, we have the freedom of choosing a distinct model from a pool of large-signal equivalent (LSE) representations, e.g., under the aspect of simplicity. The preference will be an RSL representation, which, in general, still will have a state nonlinear output function.

TABLE I
EQUIVALENT STATE TRANSFORMS AND TRANSFORMATION RULES FOR ASSOCIATED STATE FUNCTIONS

R	**Definitions**	Original State $\boldsymbol{\theta}$	Transformed State $\boldsymbol{\theta}$'
1	State Transformation	$\boldsymbol{\theta} = \mathbf{h}^{-1}(\boldsymbol{\theta}')$	$\boldsymbol{\theta}' = \mathbf{h}(\boldsymbol{\theta})$
2	Jacobian ($det(\mathbf{H}(\boldsymbol{\theta}) \neq \mathbf{0})$	$\mathbf{H}(\boldsymbol{\theta}) = \nabla_\theta \mathbf{h}(\boldsymbol{\theta})$	$\mathbf{H}(\boldsymbol{\theta}') = \nabla_\theta \mathbf{h}(\mathbf{h}^{-1}(\boldsymbol{\theta}'))$
	Transformation of Entities		
3	System State Function	$\mathbf{F}^\theta(\boldsymbol{\theta}, \mathbf{u})$	$\mathbf{F}'^\theta(\boldsymbol{\theta}', \mathbf{u}) = \mathbf{H}(\boldsymbol{\theta}')\mathbf{F}^\theta(\mathbf{h}^{-1}(\boldsymbol{\theta}'), \mathbf{u})$
4	Output Function	$\mathbf{G}^I(\boldsymbol{\theta}, \mathbf{u})$	$\mathbf{G}'^I(\boldsymbol{\theta}', \mathbf{u}) = \mathbf{G}^I(\mathbf{h}^{-1}(\boldsymbol{\theta}'), \mathbf{u})$
5	Equilibrium State Function	$\boldsymbol{\theta}^{DC}(\mathbf{u})$	$\boldsymbol{\theta}'^{DC}(\mathbf{u}) = \mathbf{h}(\boldsymbol{\theta}^{DC}(\mathbf{u}))$
6	Input Matrix	$\mathbf{B}(\mathbf{u}) = \nabla_\mathbf{u} \boldsymbol{\theta}'^{\mathbf{DC}}(\mathbf{u})$	$\mathbf{B}'(\mathbf{u}) = \mathbf{H}(\boldsymbol{\theta}^{DC}(\mathbf{u}))\mathbf{B}(\mathbf{u})$
7	Output Matrix	$\boldsymbol{\Gamma}(\mathbf{u})$	$\boldsymbol{\Gamma}'(\mathbf{u}) = \boldsymbol{\Gamma}(\mathbf{u})\mathbf{H}^{-1}(\boldsymbol{\theta}^{DC}(\mathbf{u}))$
8	Relaxation Matrix	$\mathbf{Q}_\mathbf{R}(\mathbf{u})$	$\mathbf{Q}'_\mathbf{R}(\mathbf{u}) = \mathbf{H}(\boldsymbol{\theta}^{DC}(\mathbf{u}))\mathbf{Q}_\mathbf{R}(\mathbf{u})\mathbf{H}^{-1}(\boldsymbol{\theta}^{DC}(\mathbf{u}))$
9	Delay Matrix	$\mathbf{T}_\mathbf{R}(\mathbf{u})$	$\mathbf{T}'_\mathbf{R}(\mathbf{u}) = \mathbf{H}(\boldsymbol{\theta}^{DC}(\mathbf{u}))\mathbf{T}_\mathbf{R}(\mathbf{u})\mathbf{H}^{-1}(\boldsymbol{\theta}^{DC}(\mathbf{u}))$
10	Delay Constants	$\boldsymbol{\tau}(\mathbf{u})$	$\boldsymbol{\tau}'(\mathbf{u})$
11	Eigenvector Matrix	$\mathbf{A}_R(\mathbf{u})$	$\mathbf{A}'_R(\mathbf{u}) = \mathbf{H}(\boldsymbol{\theta}^{DC}(\mathbf{u}))\mathbf{A}_R(\mathbf{u})$
12	Equilibrium Output Function	$\mathbf{i}^{DC}(\mathbf{u})$	$\mathbf{i}'^{DC}(\mathbf{u}) = \mathbf{i}^{DC}(\mathbf{u})$
13	Displacement Current	$\mathbf{i}^{DP}(\mathbf{u})$	$\mathbf{i}'^{DP}(\mathbf{u}) = \mathbf{i}^{DP}(\mathbf{u})$
14	Mode Matrices	$\mathbf{G}_k^M(\mathbf{u})$	$\mathbf{G}'^M_k(\mathbf{u}) = \mathbf{G}_k^M(\mathbf{u})$

C. Solution of Decoupled State Equations

A particular simple case is a system with decoupled states, i.e., each vector component of the system state function depends only on the respective state variable, i.e., $F_k(\boldsymbol{\theta}, \mathbf{u}) = F_k(\theta_k, \mathbf{u})$. In this case, the system can be possibly transformed into an RSL system by a state transform $\theta'_k = h_k(\theta_k)$ with a diagonal Jacobian. For each component, such a transform requires, according to Table I: R3

$$F'^\theta_k(\theta'_k, \mathbf{u}) = \frac{d\theta'_k}{d\theta_k} F^\theta_k(\theta_k, \mathbf{u}) = -\left(\theta'_k - \theta'^{\mathrm{DC}}_k(\mathbf{u})\right) \Big/ \tau_k(\mathbf{u}). \tag{20}$$

The solution of this equation is

$$\theta'_k = \theta'^{\mathrm{DC}}_k(\mathbf{u}) + \theta'_{ok} \exp\left[-\int_{\theta_{ok}}^{\theta_k} dx \Big/ \left(F^\theta_k(x, \mathbf{u})\tau_k(\mathbf{u})\right)\right] \tag{21}$$

and depends on the bias point $\mathbf{u}$. It is obvious that for an arbitrary state function, a state linearization can only be achieved in a local environment of a given bias point. Under the aspect of simplicity and speed, a model, which is globally RSL and diagonal, will always be the preferred choice from the pool of LSE representations. In this case, the time-scale transformation

$$x = \int_0^t dt' / \tau_k(\mathbf{u}(t')) \tag{22}$$

leads to an explicit analytical solution to the system equations

$$\theta_k(x) = \int_0^x e^{-(x-x')} \theta^{\mathrm{DC}}_k(x') dx' + \theta_k(0) e^{-x} \tag{23}$$

which, by insertion into (2), yields the output response for any arbitrary time-dependent input signal.

IV. LS MACROMODEL SYNTHESIS

Here, we discuss the bias-dependent SS frequency response of a nonlinear system with inner state variables and analyze the prospect of macromodel synthesis [19] from such an SS signature.

A. Bias-Dependent SS S-Parameters

Under SS conditions, the system is state linear by definition and, therefore, we cannot expect to get from an SS signature more than a state linearized truncation of the complete state–space model. The system excitation can be expressed by the input vector

$$\mathbf{u}(t) = \mathbf{u}_o + \Delta\mathbf{u}(t). \tag{24}$$

The state vectors have the form

$$\boldsymbol{\theta}(t) = \boldsymbol{\theta}^{\mathrm{DC}}(\mathbf{u}_o) + \Delta\boldsymbol{\theta}(t). \tag{25}$$

Insertion of (24) and (25) into (14) yields

$$\begin{aligned}\mathbf{i}(t) = \mathbf{i}^{\mathrm{DC}}(\mathbf{u_o}) + \nabla\mathbf{i}^{\mathrm{DC}}(\mathbf{u_o})\Delta\mathbf{u}(t) + \boldsymbol{\Gamma}(\mathbf{u_o})\Delta\boldsymbol{\theta}(t) \\ -\boldsymbol{\Gamma}(\mathbf{u_o})\nabla\boldsymbol{\theta}^{\mathrm{DC}}(\mathbf{u_o})\Delta\mathbf{u}(t) + O^2)\end{aligned} \tag{26}$$

where O^2 is a residual term of second order with respect to the input and state variables. The gradient operation is performed row wise with respect to $\mathbf{u}$ and results in an $n_I \times n_O$ matrix. Evidently, in the SS limit, the current has the form

$$\mathbf{i}(t) = \mathbf{i}^{\mathrm{DC}}(\mathbf{u_o}) + \Delta\mathbf{i}(t) \tag{27}$$

where the SS part $\Delta\mathbf{i}(t)$ depends on the time response $\Delta\boldsymbol{\theta}(t)$ resulting from (13)

$$\Delta\boldsymbol{\theta} + \mathbf{T}_R(\mathbf{u_o})\frac{d}{dt}\Delta\boldsymbol{\theta} = \nabla\boldsymbol{\theta}^{\mathrm{DC}}(\mathbf{u_o})\Delta\mathbf{u}(t) + O^2(\Delta\mathbf{u}, \Delta\boldsymbol{\theta}). \tag{28}$$

Neglecting higher order terms, we use the eigenvalue decomposition (8) of the delay matrix and solve (28) by Fourier transformation

$$\begin{aligned}\Delta\tilde{\boldsymbol{\theta}} &= (\mathbf{1}+j\omega\mathbf{T}_R(\mathbf{u_o}))^{-1}\nabla\boldsymbol{\theta}^{\mathrm{DC}}(\mathbf{u_o})\Delta\tilde{\mathbf{u}}\\ &= \mathbf{A}_R(\mathbf{u_o})(1+j\omega\boldsymbol{\tau}(\mathbf{u_o}))^{-1}\mathbf{A}_R^{-1}(\mathbf{u_o})\nabla\boldsymbol{\theta}^{\mathrm{DC}}(\mathbf{u_o})\Delta\tilde{\mathbf{u}}.\end{aligned} \tag{29}$$

Hence, in the frequency domain, SS output and input are related by the transfer function of the system

$$\begin{aligned}\mathbf{Y}(\mathbf{u}_o,\omega) = \nabla\mathbf{i}^{\mathrm{DC}}(\mathbf{u_o}) + \boldsymbol{\Gamma}(\mathbf{u_o})(j\omega\mathbf{T}_R(\mathbf{u_o}))\\ \cdot(1+j\omega\mathbf{T}_R(\mathbf{u_o}))^{-1}\mathbf{B}(\mathbf{u_o})\end{aligned} \tag{30}$$

which, in the case of the transistor, corresponds to the bias-dependent admittance matrix. In (30), we introduced the $n_s \times n_I$ input matrix

$$\mathbf{B}(\mathbf{u_o}) = \nabla\boldsymbol{\theta}^{\mathrm{DC}}(\mathbf{u_o}). \tag{31}$$

In terms of the input, output, and relaxation matrix, the transfer function has the form well known from linear control theory (see, e.g., [7, p. 35]). In the considered nonlinear case, the input matrix is given as a gradient of an equilibrium state function.

B. Mode Matrices and Factorization

With use of (8), the transfer function can also be written in the so-called pole-residue form [19]

$$\mathbf{Y}(\mathbf{u_o},\boldsymbol{\omega}) = \mathbf{G_o^M}(\mathbf{u_o}) + \sum_{n=1}^{n_s}\mathbf{G_n^M}(\mathbf{u_o})(1+j\omega\tau_n(\mathbf{u_o}))^{\mathbf{-1}} \tag{32}$$

where we have introduced the frequency-independent mode matrices ($n \geq 1$)

$$G_{nik}^M = \left(\mathbf{G}_n^M\right)_{ik} = \sum_{l=1}^{n_s}(\boldsymbol{\Gamma})_{il}(\mathbf{A}_R)_{ln}\sum_{m=1}^{n_s}(\mathbf{A}_R)_{nm}^{-1}(\mathbf{B})_{mk} \tag{33}$$

$$\mathbf{G}_{\mathbf{o}}^M = \nabla\mathbf{i}^{\mathrm{DC}} - \sum_{n=1}^{n_s}\mathbf{G}_{\mathbf{n}}^M. \tag{34}$$

Equation (32) means that the admittance matrix can be presented as a sum of n_s+1 matrix terms (modes) each of which is characteristic for a specific state variable with a respective delay time. The transit mode matrix $\mathbf{G}_o^M(\mathbf{u_o})$ describes the system at infinite frequency. The mode matrices $\mathbf{G}_n^M(\mathbf{u_o})$ are real valued if all delay times are real valued. By inspection of (33), we see that the mode matrix coefficients $G_{nik}^M = (\mathbf{G}_n^M)_{ik}$ satisfy the factorization conditions

$$G_{nik}^M = \gamma_{\mathrm{in}}^o(\mathbf{u_o})b_{nk}^o(\mathbf{u_o}). \tag{35}$$

In the case of a two-port device, the factorization conditions (35) mean that the determinant of each mode matrix has to vanish (for $1 \leq n \leq n_s$)

$$\det\left(\mathbf{G_n^M}(\mathbf{u_o})\right) = G_{n11}^M G_{n22}^M - G_{n12}^M G_{n21}^M = 0. \tag{36}$$

If two modes have identical delay times, a unique mode assignment is no longer possible. Apparent violations of the factorization conditions may occur in this degenerate case.

C. Factor Reconstruction

We now investigate the feasibility to retrieve the original state linear equations (13) and (14) from a complete S-parameter data set (from which the admittance matrix data can be calculated). The goal is to identify the number of system modes, their equilibrium state function, the delay matrix, and the output matrix, all of which may be bias dependent. To achieve this goal, we will have to pass through the following five steps.

Step 1) Determination of mode matrices and delays.
Step 2) Preparation of input and output factors.
Step 3) Finding a valid eigenvector matrix.
Step 4) Setting up a special state representation.
Step 5) Tailoring the state representation.

We suppose—by appropriate analysis of the frequency dependence of the admittance matrix—we have determined a unique set of delay times $\boldsymbol{\tau}(\mathbf{u_o})$ and respective mode matrices $\mathbf{G}_m^M(\mathbf{u_o})$ [Step 1)]. The goal is to determine the state functions on the basis of (33).

For this purpose, we have to construct output factors $\gamma_{\mathrm{in}}^o(\mathbf{u_o})$ and input factors $b_{nk}^o(\mathbf{u_o})$ from the mode matrices according to (35) in Step 2). For each mode n, we select a column k_n and a row i_n for which $G_{ni_nk_n}^M(\mathbf{u_o}) \neq \mathbf{0}$ is in the entire ROI, and obtain the input factors

$$b_{nk}^o(\mathbf{u_o}) = b_{nk_n}^o(\mathbf{u_o})\, G_{ni_nk}^M(\mathbf{u_o}) \big/ G_{ni_nk_n}^M(\mathbf{u_o}). \tag{37}$$

One of the four factor elements of each mode matrix can be set to an arbitrary value, hence, we can generate a special set with smooth bias dependence by choosing $b_{nk_n}^o(\mathbf{u_o}) = 1$. With this choice, we readily obtain all remaining output factors

$$\gamma_{\mathrm{in}}^o(\mathbf{u_o}) = G_{nik}^M(\mathbf{u_o}) \big/ b_{nk}^o(\mathbf{u_o}). \tag{38}$$

D. Valid Eigenvector Matrices and State Functions

Unfortunately, the reconstruction of the state equations is not straightforward since the definition (35) of the mode factors results in matrices $\mathbf{B_o}(\mathbf{u_o})$ and $\boldsymbol{\Gamma}_o(\mathbf{u_o})$, which are not unique. The undetermined norm of the eigenvectors in the matrix $\mathbf{A_R}(\mathbf{u_o})$ allows for multiplication with a diagonal matrix $\mathbf{D}(\mathbf{u_o})$. The constructed mode factors are related to the input matrix of (31) and the output matrix (11) according to

$$\mathbf{B_o}(\mathbf{u_o}) = \mathbf{D^{-1}}(\mathbf{u_o})\mathbf{A_R^{-1}}(\mathbf{u_o})\mathbf{B}(\mathbf{u_o}) = \mathbf{A^{-1}}(\mathbf{u_o})\mathbf{B}(\mathbf{u_o}) \tag{39}$$

$$\boldsymbol{\Gamma}_o(\mathbf{u_o}) = \boldsymbol{\Gamma}(\mathbf{u_o})\mathbf{A_R}(\mathbf{u_o})\mathbf{D}(\mathbf{u_o}) = \boldsymbol{\Gamma}(\mathbf{u_o})\mathbf{A}(\mathbf{u_o}) \tag{40}$$

and input and output matrices apparently can be determined only within a class of invertible matrix transformations $\mathbf{A}(\mathbf{u_o})$. However, the variation of the eigenvectors with bias matters since the output matrix $\mathbf{B}(\mathbf{u_o})$ has to satisfy (31). Solving (39) and (40) for $\mathbf{B}(\mathbf{u_o})$ and $\boldsymbol{\Gamma}(\mathbf{u_o})$ and inserting (31), we get the

following relation between the bias dependent set of factors $\gamma^o_{\rm in}$ and b^o_{nk} and the state functions:

$$\frac{\partial}{\partial u_k}\boldsymbol{\theta}^{\rm DC}_n(\mathbf{u}) = \sum_{m=1}^{n_s} A_{nm}(\mathbf{u_o}))b^o_{mk}(\mathbf{u}) \tag{41}$$

$$(\mathbf{T}_R(\mathbf{u_o}))_{\rm in} = \sum_{m=1}^{n_s} A_{im}(\mathbf{u_o})))\tau_m(\mathbf{u_o})A^{-1}_{mn}(\mathbf{u_o})) \tag{42}$$

$$(\mathbf{\Gamma}(\mathbf{u_o}))_{\rm in} = \sum_{m=1}^{n_s} \gamma^o_{im}(\mathbf{u_o})A^{-1}_{mn}(\mathbf{u_o}))). \tag{43}$$

For a given set of coefficients $b^o_{mk}(\mathbf{u}_o)$, (41) constitutes a condition for the otherwise unrestricted nonsingular matrix function $\mathbf{A}(\mathbf{u}_o)$. If $\mathbf{A}(\mathbf{u}_o)$ is a solution of (41), it is a valid eigenvector matrix $\mathbf{A}(\mathbf{u_o}) = \mathbf{A_R}(\mathbf{u_o})$, and we obtain the state functions $\mathbf{\Gamma}(\mathbf{u})$ from (43), $\mathbf{Q}_R(\mathbf{u}) = \mathbf{T}^{-1}_R(\mathbf{u})$ from (42), and $\nabla\boldsymbol{\theta}^{\rm DC}(\mathbf{u})$ from (41) as a special state representation of the state linearized system [Step 4)]. The equilibrium state functions $\boldsymbol{\theta}^{\rm DC}(\mathbf{u})$ are determined from $\nabla\boldsymbol{\theta}^{\rm DC}(\mathbf{u})$ (as path independent result) by path integration.

For the state–space reconstruction, we first need to find a valid eigenvector matrix [Step 3)] as given by (41), which forms a set of $n_s \times n_I$ equations for $n_s \times n_s$ unknown matrix elements $A_{nm}(\mathbf{u_o})$. We point out two approaches of finding a special solution of (41). A direct algebraic solution is possible if there are at least as many state variables as input variables. In this case, we may zero $n_s(n_s - n_I)$ matrix elements and solve the linear equation (41) for the remaining matrix elements. Surprisingly, there is a free choice of the equilibrium state functions $\boldsymbol{\theta}^{\rm DC}(\mathbf{u})$ unless the factorizing coefficients b^o_{nk} are ill conditioned.

For the other approach, we differentiate (41) with respect to the input variables and find that an equilibrium state function that satisfies (31) exists if and only if the matrix $\mathbf{A}(\mathbf{u})$ satisfies the integrability conditions

$$\frac{\partial}{\partial u_i}\sum_{m=1}^{n_s} A_{nm}(\mathbf{u})b^o_{mj}(\mathbf{u}) = \frac{\partial}{\partial u_j}\sum_{m=1}^{n_s} A_{nm}(\mathbf{u})b^o_{mi}(\mathbf{u}). \tag{44}$$

Equation (44) represents a quasi-linear system of n_s partial differential equations (PDEs) (with respect to the n_I input variables) for the $n_s \times n_s$ matrix $\mathbf{A}(\mathbf{u}_o)$ with a manifold of solutions.

The second solution approach is to choose the matrix $\mathbf{A}(\mathbf{u}_o)$ to be diagonal. Upon temporary suppression of the state variable index, for each state variable, (41) reads $\nabla\theta^{\rm DC}(\mathbf{u}) = A(\mathbf{u})\mathbf{b}^o(\mathbf{u})$, i.e., the row vector $\mathbf{b}^o(\mathbf{u})$ defines the direction of the gradient of $\theta^{\rm DC}$. For a two-port, we can eliminate $A(\mathbf{u})$ to obtain the equivalent equation

$$\nabla\theta^{\rm DC}(\mathbf{u}) \cdot \mathbf{b}^o_\perp(\mathbf{u}) = 0 \tag{45}$$

where $\mathbf{b}^o_\perp(\mathbf{u}) = (b^o_2(\mathbf{u}), -b^o_1(\mathbf{u}))$ The PDE (45) defines the contour lines of constant $\theta^{\rm DC}$. The general invariance with respect to nonlinear state transforms leaves the freedom to assign a value of the state variable to each contour line of the equilibrium state function. Alternatively to (41), we may solve the integrability equation (44), i.e.,

$$b^o_1(\mathbf{u})\frac{\partial p(\mathbf{u})}{\partial u_2} - b^o_2(\mathbf{u_o})\frac{\partial p(\mathbf{u})}{\partial u_1} = \frac{\partial b^o_2(\mathbf{u})}{\partial u_1} - \frac{\partial b^o_1(\mathbf{u})}{\partial u_2} \tag{46}$$

where $p(\mathbf{u}) = \ln(A(\mathbf{u}))$.

E. Manifold of SSE Models

The whole manifold of state-linear models showing the same SS signature is obtained as the manifold of solutions for (41) or (44) spanned by the variety of consistent boundary conditions. The following operation will enable us to generate this manifold from a single initial model reproducing the SS signature. First, we employ a nonlinear state transform (17) and obtain a new representation, which is exactly equivalent, but nonlinear in the state variables. Next, we state linearize the new representation and obtain a new state-linear model with exactly the same SS signature. From Table I, we see that such SSE state transformations can be expressed in terms of a bias-dependent matrix $\mathbf{H}(\mathbf{u})$, which transforms the input, output, and relaxation matrices. However, since the equilibrium state function is retained upon state linearization, the matrix $\mathbf{H}(\mathbf{u})$ cannot be chosen completely arbitrarily, but similar to the matrix $\mathbf{A}(\mathbf{u})$ in (41), it has to obey a subtle integrability condition. According to Table I: R6–R11, the transformation with the Jacobian $\mathbf{H}(\boldsymbol{\theta}^{\rm DC}(\mathbf{u})) = \nabla_\theta\mathbf{h}(\boldsymbol{\theta}^{\rm DC}(\mathbf{u}))$ of the state transform leaves the mode matrices unaffected. Also by construction (owing to Table I: R5), the state transform maintains the integrability condition (41) and (44). Vice versa, any solution of (41) can be traced to a transform $\boldsymbol{\theta}' = \mathbf{h}(\boldsymbol{\theta})$ of the special representation. Due to (39), any other solution $\mathbf{A}'(u), \boldsymbol{\theta}'^{\rm DC}(\mathbf{u})$ of (41) is related to the functions $\mathbf{A}(\mathbf{u}), \boldsymbol{\theta}^{\rm DC}(\mathbf{u})$ of the special representation by

$$\nabla\boldsymbol{\theta}'^{\rm DC}(\mathbf{u}) = \mathbf{A}'(\mathbf{u})\mathbf{A^{-1}}(\mathbf{u})\nabla\boldsymbol{\theta}^{\rm DC}(\mathbf{u}) = \mathbf{A}''(\mathbf{u})\nabla\boldsymbol{\theta}^{\rm DC}(\mathbf{u}) \tag{47}$$

(given the matrices $\mathbf{A}(\mathbf{u})$ and $\mathbf{A}'(\mathbf{u})$ are nonsingular in the entire ROI). We turn the function $\mathbf{A}(\mathbf{u})$ into a function of the state variables by assigning to each bias point the respective values given by the equilibrium function $\boldsymbol{\theta}^{\rm DC}(\mathbf{u})$. By path integration of the transformation matrix,

$$\boldsymbol{\theta}'^{\rm DC}(\mathbf{u}) = \int_{\mathbf{u_R}}^{\mathbf{u}} \mathbf{A}''(\mathbf{u}')\nabla\boldsymbol{\theta}^{\rm DC}(\mathbf{u}')\,\mathbf{du}' = \int_{\boldsymbol{\theta}^{\mathbf{DC}}(\mathbf{u_R})}^{\boldsymbol{\theta}^{\mathbf{DC}}(\mathbf{u})} \mathbf{H}(\boldsymbol{\theta}')\,\mathbf{d}\boldsymbol{\theta}' \tag{48}$$

and with use of transformation rule Table I: R5, we have established the functional relation $\boldsymbol{\theta}' = \mathbf{h}(\boldsymbol{\theta})$ between the old and new state representation. For an arbitrary matrix $\mathbf{A}''(\mathbf{u}')$, the integral still depends on the path, but for a proper choice in accordance with Table I: R2, it becomes path independent. Yet a valid SSE transformation matrix can be obtained from an arbitrary nonsingular matrix $\mathbf{A}''(\mathbf{u}')$ and an arbitrary convention of the path integration by performing (48) to establish the LSE state transform and subsequently carrying out the gradient operation on the obtained new equilibrium function.

F. Consequences and Construction Strategies

It is interesting to note that, for a transistor two-port, there always exists a *diagonal* state-linear model, which is consistent with its SS signature. If there are at least two state variables, we can apply the algebraic solution approach to solve (41) and choose the port voltages (or combinations of them) as equilibrium state functions. We then use the obtained eigenvector matrix $\mathbf{A_R}(\mathbf{u})$ as matrix $\mathbf{A}''(\mathbf{u})$ in (48) to construct an equivalent state transform by path integration of the equilibrium state function. By construction, the new state representation has a diagonal relaxation matrix.

Hence, for a well-conditioned system , there always exists a transformation, which diagonalizes the relaxation matrix for *all* bias conditions, yet this state representation is not unique. The set of all state-linear and diagonal models can also be obtained directly by solving the contour (45) or (46) for a diagonal state representation. As discussed in Section IV-D for the contour lines of the equilibrium state, there still remain n_S degrees of freedom for nonlinear expansions and contractions along the diagonal state axes associated with a spectrum of respective state functions.

In the state-linear limit, all these diagonal state representations are mutually equivalent. However, state linearity is lost upon any LSE state transformation (17) and there is a clear difference between state–space representations under LS excitation when quadratic state terms become important [see (5) and (10)]. This difference can be used for an individual nonlinear readjustment of the scale for each state variable to maintain state linearity for LS conditions.

The considered SSE transforms have the potential to prepare an optimum state-linear model. However, in general, they will not be able to prepare an optimum RSL model since this possibly possesses a state-nonlinear output function. Please note that any state model leaves the free choice of setting up the linear scales for the state variables. Gain and offset constants of each individual scale remain to be defined, e.g., by assigning appropriate values to the equilibrium state function at convenient bias points.

V. LS Approach for the HEMT Standard Equivalent Circuit

In the following, we construct a global LS extension for the SS standard equivalent circuit of the FET (Fig. 1), which consists of bias-dependent lumped elements. The intrinsic admittance matrix can be written as

$$\mathbf{Y} = \begin{pmatrix} Y_{\rm GS}+Y_{\rm GD} & -Y_{\rm GD} \\ Y_{\rm GM}-Y_{\rm GD} & Y_{\rm DS}+Y_{\rm GD} \end{pmatrix}. \tag{49}$$

Each of the subunits in Fig. 1(b) can be assigned to a distinct system mode and be described by three constants, i.e.: 1) an LF conductivity $g^{\rm DC}$; 2) an HF conductivity $g^{\rm HF}$; and 3) a time constant τ. We can use the identity

$$g^{\rm HF}+\frac{g^{\rm DC}-g^{\rm HF}}{1+j\omega\tau} = g^{\rm DC}+\frac{j\omega C}{1+j\omega\tau} = \frac{g^{\rm DC}+j\omega C'}{1+j\omega\tau} \tag{50}$$

where $g^{\rm HF} = g^{\rm DC} + C/\tau = C'/\tau$ to eliminate all capacitors from the LS model. By assuming a very small value for $\tau_{\rm DS}$, the effect of a drain capacity is emulated by the dispersion of the output conductance. The combined effects of the transit time of the current source and the delay of the control voltage are approximated by a mode with the delay time $\tau_{\rm GM}$. Since each component in (49) is of the form (50), in Step 1) (with $\Delta g = g^{\rm DC}-g^{\rm HF}$)), we directly obtain the mode matrix decomposition (32)

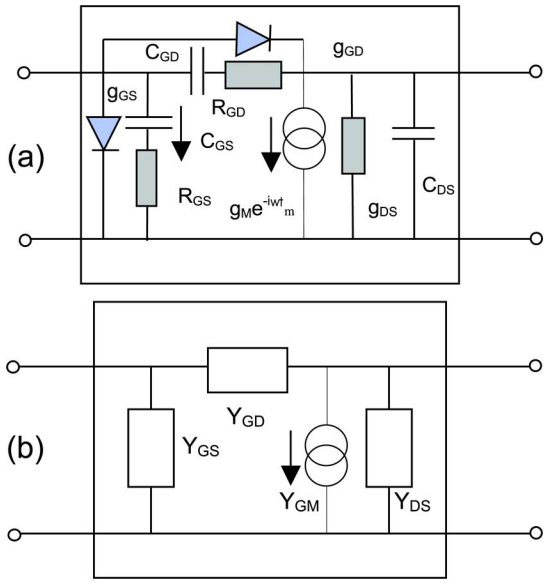

Fig. 1. Equivalent circuit of the HEMT as composed: (a) by lumped elements and (b) by block elements.

$$\mathbf{G_{GS}} = \begin{pmatrix} \Delta g_{\rm GS} & 0 \\ 0 & 0 \end{pmatrix} \tag{51}$$

$$\mathbf{G}_{\rm GD} = \begin{pmatrix} \Delta g_{\rm GD} & -\Delta g_{\rm GD} \\ -\Delta g_{\rm GD} & \Delta g_{\rm GD} \end{pmatrix}$$

$$\mathbf{G}_{\rm GM} = \begin{pmatrix} 0 & 0 \\ \Delta g_M & 0 \end{pmatrix}$$

$$\mathbf{G}_{\rm DS} = \begin{pmatrix} 0 & 0 \\ 0 & \Delta g_{\rm DS} \end{pmatrix}$$

$$\mathbf{G_o} = \begin{pmatrix} g^{\rm HF}_{\rm GS}+g^{\rm HF}_{\rm GD} & -g^{\rm HF}_{\rm GD} \\ -g^{\rm HF}_{\rm GD} & g^{\rm HF}_{\rm DS}+g^{\rm HF}_{\rm GD} \end{pmatrix}. \tag{52}$$

A factorization [Step 2)] of the mode matrices is given by

$$\mathbf{\Gamma}^o(\mathbf{u}) = \begin{pmatrix} \Delta g_{\rm GS}(\mathbf{u}) & \Delta g_{\rm GD}(\mathbf{u}) & 0 & 0 \\ 0 & -\Delta g_{\rm GD}(\mathbf{u}) & \Delta g_M(\mathbf{u}) & \Delta g_{\rm DS}(\mathbf{u}) \end{pmatrix} \tag{53}$$

$$\mathbf{B}^{oT}(\mathbf{u}) = \begin{pmatrix} 1 & 1 & 1 & 0 \\ 0 & -1 & 0 & 1 \end{pmatrix}. \tag{54}$$

In the Step 3), we would have to select eight nonzero elements of the 4×4 eigenvector matrix and set up the linear equations for the algebraic solution of (41). However, the simple form of $\mathbf{B}^o(\mathbf{u})$ facilitates direct integration and yields the unity matrix as an eigenvector matrix. The output matrix is given by (53) and

the equilibrium state functions are simple combinations of the port voltages [Step 4)]

$$\boldsymbol{\theta}^{\mathrm{DC}}(\mathbf{u}) = (\mathrm{U_{GS}}, \quad U_{\mathrm{GS}} - U_{\mathrm{DS}}, \quad U_{\mathrm{GS}}, \quad U_{\mathrm{DS}}). \tag{55}$$

The state variables correspond to delayed voltages with the diagonal delay matrix

$$\mathbf{T_R}(\mathbf{u}) = \begin{pmatrix} \tau_{\mathrm{GS}}(\mathbf{u}) & 0 & 0 & 0 \\ 0 & \tau_{\mathrm{GD}}(\mathbf{u}) & 0 & 0 \\ 0 & 0 & \tau_{\mathrm{GM}}(\mathbf{u}) & 0 \\ 0 & 0 & 0 & \tau_{\mathrm{DS}}(\mathbf{u}) \end{pmatrix}. \tag{56}$$

If the system description is correct, the mode matrices should satisfy the condition

$$\nabla \mathbf{i}^{\mathrm{DC}}(\mathbf{u}) = \mathbf{G_o}(\mathbf{u}) + \mathbf{G_{GS}}(\mathbf{u}) + \mathbf{G_{GD}}(\mathbf{u}) + \mathbf{G_{GM}}(\mathbf{u}) + \mathbf{G_{DS}}(\mathbf{u}). \tag{57}$$

Insertion of the state functions (53) and (55)–(57) into (13) and (14) yields an LS model, which is consistent with the SSE circuit of Fig. 1 over the entire bias range. No additional assumptions have to be made about the conductances, which define the system by (52) and (53) and contain the gate charge functions, implicitly.

VI. LFD

LFD leads to a situation where the extrapolated LF limit of the admittance matrix deviates from the dc admittance and (57) is apparently violated. This deviation has to be attributed to additional system modes with large time constants so that the respective dispersion is not observed in the investigated frequency range with the lower limit ω_{LF}.

A. Separation of the LFD Modes

It is convenient to introduce an LFD matrix as the difference

$$\mathbf{Y}(\mathbf{u_o}, \mathbf{0}) - \mathbf{Y}(\mathbf{u_o}, \omega_{\mathrm{LF}}) \approx \sum_{n=1}^{n_{\mathrm{LF}}} \mathbf{G}_n^{\mathbf{M}}(\mathbf{u_o}) = \mathbf{G}^{\mathrm{LFD}}(\mathbf{u_o}). \tag{58}$$

The dispersion matrix may be composed of several components, which, in principle, can be resolved by S-parameter measurements at LF. However, if such information is not available, we may assume that there is only a single dispersion mode or that the dispersion modes are degenerate. Since the delay constant $\tau_{\mathrm{LF}}(\mathbf{u}_o)$ of LFD is not known exactly, commonly an estimated voltage-independent value is used.

If (and only if) there is no coupling between HF and LF dispersive modes, then there are two separate sets of state equations (13) for the LF and HF modes and the output matrix, i.e.,

$$\boldsymbol{\Gamma}(\mathbf{u_o}) = \left(\boldsymbol{\Gamma}^{\mathrm{HF}}(\mathbf{u_o}), \boldsymbol{\Gamma}^{\mathrm{LF}}(\mathbf{u_o})\right) \tag{59}$$

$$\mathbf{B}(\mathbf{u_o}) = \begin{pmatrix} \mathbf{B}^{\mathrm{HF}}(\mathbf{u_o}) \\ \mathbf{B}^{\mathrm{LF}}(\mathbf{u_o}) \end{pmatrix}. \tag{60}$$

For each LF mode, we have to add an extra row $\mathbf{b}_n(\mathbf{u}_o)$ in the input matrix and an extra column $\boldsymbol{\gamma}_n(\mathbf{u}_o)$ in the output matrix

$$\boldsymbol{\Gamma}^{\mathrm{LF}}(\mathbf{u_o}) = \left(\boldsymbol{\gamma}_1^{\mathrm{LF}}(\mathbf{u_o}), \boldsymbol{\gamma}_2^{\mathrm{LF}}(\mathbf{u_o}), \ldots\right) \tag{61}$$

$$\mathbf{B}^{\mathrm{LF}}(\mathbf{u_o}) = \left(\mathbf{b}_1^{\mathrm{LF}}(\mathbf{u_o}), \mathbf{b}_2^{\mathrm{LF}}(\mathbf{u_o}), \ldots\right)^T. \tag{62}$$

For an LS model, the input matrix has to equal the gradient of the equilibrium function according to (31)

$$\mathbf{B}^{\mathrm{LF}}(\mathbf{u_o}) = \boldsymbol{\nabla\theta}^{\mathrm{LFDC}}(\mathbf{u_o}) \tag{63}$$

and from the state-linear approach (30), we obtain the following SS relation between the (measured) LFD matrix and (sought) state functions:

$$\mathbf{G}^{\mathrm{LFD}}(\mathbf{u_o}) = \boldsymbol{\Gamma}^{\mathrm{LF}}(\mathbf{u_o}) \nabla \boldsymbol{\theta}^{\mathrm{LFDC}}(\mathbf{u_o}). \tag{64}$$

The respective state-linear output equations are

$$\begin{aligned} \mathbf{i} &= \mathbf{i}^{\mathbf{DC}}(\mathbf{u}) + \boldsymbol{\Gamma}^{\mathrm{HF}}(\mathbf{u})(\boldsymbol{\theta}^{\mathrm{HF}} - \boldsymbol{\theta}^{\mathrm{HFDC}}(\mathbf{u})) \\ &\quad + \boldsymbol{\Gamma}^{\mathrm{LF}}(\mathbf{u})(\boldsymbol{\theta}^{\mathrm{LF}} - \boldsymbol{\theta}^{\mathrm{LFDC}}(\mathbf{u})) \\ &= \mathbf{i}^{\mathbf{o}}(\mathbf{u}) + \boldsymbol{\Gamma}^{\mathrm{LF}}(\mathbf{u})(\boldsymbol{\theta}^{\mathrm{LF}} - \boldsymbol{\theta}^{\mathrm{LFDC}}(\mathbf{u})). \end{aligned} \tag{65}$$

If the input signal contains only (harmonic) frequency components well above the LFD frequency $1/\tau^{\mathrm{LF}}(\mathbf{u})$, then the state variable is nearly constant even in LS operation ("frozen state"). If (and only if) we have an RSL representation, then according to (13), the state variable is close to the time average

$$\boldsymbol{\theta}^{\mathrm{LF}} \approx \overline{\boldsymbol{\theta}^{\mathrm{LFDC}}(\mathbf{u})}. \tag{66}$$

B. Single-Mode LFD Models

It is common practice to approximate the LFD by a single mode (dispersion model of Root [12], [20]) with the properties

$$\mathbf{G}^{\mathrm{LFD}}(\mathbf{u_o}) = \begin{pmatrix} 0 & 0 \\ \dfrac{\partial}{\partial u_1}\theta^{\mathrm{LFDC}}(\mathbf{u_o}) & \dfrac{\partial}{\partial u_2}\theta^{\mathrm{LFDC}}(\mathbf{u_o}) \end{pmatrix} \tag{67}$$

i.e.,

$$\mathbf{b}^{\mathrm{LF}}(\mathbf{u_o}) = \nabla\theta^{\mathrm{LFDC}}(\mathbf{u_o}) \tag{68}$$

$$\boldsymbol{\gamma}^{\mathrm{LF}}(\mathbf{u_o}) = (0 \quad 1). \tag{69}$$

The Root model postulates the existence of a primitive state function for the drain current at the LF limit ω_{LF} and that the LFD matrix satisfies corresponding integrability conditions. It can be shown that even if (67) is not satisfied globally, there still exists a state function that matches the LFD matrix exactly along a given straight or bent line $u_2 = f_{Ro}(u_1)$ intersecting the (u_1, u_2)-bias plane. However, deviations of the voltage trajectories from such a line may be considerable and pose a problem for global LS models.

We now discuss two extensions of the Root model, which are globally compatible with the LFD matrix. If there is only a single mode, we begin with $\gamma_k^{o\mathrm{LF}}(\mathbf{u_o}) = \delta_{2k}$ and $b_k^{o\mathrm{LF}}(\mathbf{u_o}) =$

$\mathbf{G_k^{LFD}}(\mathbf{u_o})$ and solve the PDE (46) for a single bias-dependent transformation element $A(\mathbf{u}_o)$. With any regular solution ($A(\mathbf{u}_o) \neq 0$ in the ROI) of this equation, we have the output matrix

$$\mathbf{\Gamma}^{\mathrm{LF}}(\mathbf{u}) = \begin{pmatrix} 0 \\ A(\mathbf{u}) \end{pmatrix} \tag{70}$$

and obtain the equilibrium function of the LFD state by path integration

$$\boldsymbol{\theta}^{\mathrm{LFDC}}(\mathbf{u}) = \int_{\mathbf{u_R}}^{\mathbf{u}} [b^o_{\mathrm{LF}}(\mathbf{u}')/\, A(\mathbf{u}')]\, d\mathbf{u}'. \tag{71}$$

This equation looks similar to the path integration used for the Root model (with $A(\mathbf{u}_o) = 1$), but now by construction yields a path-independent result. In practice, construction of the dispersion equilibrium state function on the basis of the PDEs (45) or (46) turns out to be difficult since complications arise in regions where all elements of the dispersion mode matrix are close to zero.

C. Double-Mode LFD Models

These problems can be circumvented by another extension of the simple Root model, which is based on the assumption that there are two LFD modes with the same or similar delay constants. For the state-linearized system, we make the approach

$$\boldsymbol{\theta}^{\mathrm{LFDC}}(\mathbf{u}) = \begin{pmatrix} \theta_1^{\mathrm{LFDC}}(\mathbf{u}) \\ \theta_2^{\mathrm{LFDC}}(\mathbf{u}) \end{pmatrix} \tag{72}$$

$$\mathbf{\Gamma}^{\mathrm{LF}}(\mathbf{u}) = \begin{pmatrix} 0 & 0 \\ 1 & \mathbf{e}\cdot\mathbf{u} \end{pmatrix} \tag{73}$$

where the unit vector $\mathbf{e} = (\cos\varphi, \sin\varphi)$ defines a preferential axis in the bias plane. This double current state (DCS) approach yields the LFD mode matrix

$$\mathbf{G}^{\mathrm{LFD}}(\mathbf{u}) = \begin{pmatrix} \vec{0} \\ \nabla\theta_1^{\mathrm{LFDC}}(\mathbf{u}) + (\mathbf{e}\cdot\mathbf{u})\nabla\boldsymbol{\theta}_2^{\mathrm{LFDC}}(\mathbf{u}) \end{pmatrix}. \tag{74}$$

The basic idea of the DCS approach is to use the identity

$$\begin{aligned} &\nabla\theta_1^{\mathrm{LFDC}}(\mathbf{u}) + (\mathbf{e}\cdot\mathbf{u})\nabla\boldsymbol{\theta}_{\mathbf{1}}^{\mathrm{LFDC}}(\mathbf{u})) \\ &\quad = \nabla(\theta_1^{\mathrm{LFDC}}(\mathbf{u}) + (\mathbf{e}\cdot\mathbf{u})\theta_{\mathbf{1}}^{\mathrm{LFDC}}(\mathbf{u})) - \boldsymbol{\theta}_{\mathbf{2}}^{\mathrm{LFDC}}(\mathbf{u})\nabla(\mathbf{e}\cdot\mathbf{u}) \end{aligned} \tag{75}$$

and to choose a direction for the path integral where the second term vanishes. For the special case $\varphi = 90°$, i.e., $\mathbf{e}\cdot\mathbf{u} = \boldsymbol{u_2}$, we have

$$G_{21}^{\mathrm{LFD}} = \frac{\partial}{\partial u_1}\left(\theta_1^{\mathrm{LFDC}} + u_2\theta_2^{\mathrm{LFDC}}\right) \tag{76}$$

$$G_{22}^{\mathrm{LFD}} = \frac{\partial}{\partial u_2}\left(\theta_1^{\mathrm{LFDC}} + u_2\theta_2^{\mathrm{LFDC}}\right) - \theta_2^{\mathrm{LFDC}}. \tag{77}$$

The first equation is readily integrated [with the freedom to choose an additive function $y(u_2)$] and yields the first summand of the second equation, which then can be resolved for the second state function. Resubstitution into the first equation yields the first state function. The same procedure works for any direction of the unit vector $\mathbf{e}$ by path integration along the direction orthogonal to $\mathbf{e}$.

For the dispersion models discussed above, assumptions about the output matrix were made and the equilibrium state function was derived in turn. We now investigate the opposite option of choosing an equilibrium state function first and finding a suitable output matrix. It is a surprising fact that there is a free choice for the equilibrium functions under the premises that: 1) there are two dispersion modes and 2) their equilibrium functions are invertible. Under these conditions, (64) can always be inverted as follows:

$$\mathbf{\Gamma}^{\mathrm{LF}}(\mathbf{u}) = \Delta\mathbf{G}^{\mathbf{M}}(\mathbf{u})(\nabla\boldsymbol{\theta}^{\mathrm{LFDC}}(\mathbf{u}))^{-\mathbf{1}}. \tag{78}$$

The simplest choice for the equilibrium functions, which complies with these requirements, is

$$\boldsymbol{\theta}^{\mathrm{LFDC}}(\mathbf{u}) = (u_1, u_2) \tag{79}$$

and results in a voltage lag model [21] with

$$\mathbf{B}(\mathbf{u}) = 1 \tag{80}$$

$$\mathbf{\Gamma}(\mathbf{u_o}) = \mathbf{G}^{\mathrm{LFD}}(\mathbf{u}). \tag{81}$$

The assumption of two LFD modes is plausible in view of distinct gate and drain lag effects [14]. These effects are thought to arise from charges at deep traps, which are located on the drain side and the source side of the gate and which are influenced by the bias conditions.

D. Analytic Comparison of LFD Models

It is interesting to compare the analytical expressions obtained with the voltage lag model (80), (81) and the Root model (68), (69). Under the assumption that (63) is satisfied, both models will generate identical S-parameter data. Under LS conditions (such as load–pull experiments) with negligible LF input signal components, according to (66) the Root model predicts

$$i_{\mathrm{DS}} = i_{o\mathrm{DS}}(\mathbf{u}) + (\overline{\boldsymbol{\theta}^{\mathrm{LFDC}}(\mathbf{u})} - \boldsymbol{\theta}^{\mathrm{LFDC}}(\mathbf{u})) \tag{82}$$

whereas the two-mode voltage lag model yields

$$i_{\mathrm{DS}} = i_{o\mathrm{DS}}(\mathbf{u}) + \nabla\boldsymbol{\theta}^{\mathrm{LFDC}}(\mathbf{u})(\bar{\mathbf{u}} - \mathbf{u}). \tag{83}$$

The predictions of the two models clearly differ as soon as the nonlinearity of the function $\theta^{\mathrm{LFDC}}(\mathbf{u})$ has to be taken into account.

Finally, we exemplify the effect of the equivalent state transform (17) with the Root model. By application of (17) and neglect of higher order terms, we have the most general state-linear one-mode LFD model for the special LFD matrix (67) satisfying the integrability constraint. With use of Table I: R7, it yields the LS response

$$i_{\mathrm{DS}} = i_{o\mathrm{DS}}(\mathbf{u}) + \frac{\overline{h(\theta^{\mathrm{LFDC}}(\mathbf{u}))} - h(\theta^{\mathrm{LFDC}}(\mathbf{u}))}{\dfrac{d}{d\theta^{\mathrm{LF}}}h(\theta^{\mathrm{LFDC}}(\mathbf{u}))}. \tag{84}$$

The scalar function $h(\theta^{\mathrm{LF}})$ is arbitrary, but has to be either globally monotonic increasing or decreasing.

E. Power-Sweep Simulations

In the following, we want to exemplify the effect and usefulness of SSE transforms by comparison of model prediction with experimental data for a transistor in LS operation. A GaN power HEMT with eight fingers and a total gatewidth of 480 μm was stimulated at 2 GHz under class AB conditions $(\overline{u_{\rm GS}}, \overline{u_{\rm DS}}) = (-3\,{\rm V}, 26\,{\rm V})$, and the microwave power consumed at an ohmic output load of 50 Ω was measured in dependence of the input power. Simultaneous measurements of the components of the input and output voltage waves up to the ninth harmonic order facilitated the reconstruction of the current and voltage trajectories in the time domain. A rhomboidal-shaped region was filled by the voltage trajectories implying that a suitable LS model should at least cover the voltage range $-8\,{\rm V} < u_{\rm gs} < 2\,{\rm V}$ and $17\,{\rm V} < u_{\rm ds} < 35\,{\rm V}$.

The influence of LFD phenomena on the performance of this transistor was shown by dc-pulse measurements, which showed a pronounced variation of the output characteristics with the quiescent bias. To built a state-of-the-art LS HEMT model, a complete S-parameter set was measured in the frequency range from 300 MHz to 20 GHz for a bias list covering the ROI. The model obtained from this SS database comprises the elements of the parasitic network, the voltage-dependent charge, and delay functions and current functions for the dc input and output currents. Output conductance and transconductance as extrapolated from the S-parameter measurements clearly did not form the complete differential (67), as required for the Root model, since the transfer characteristics (at any $V_{\rm ds}$ above the knee voltage) consistently showed an SS gain, which was consistently smaller, and an output conductance, which was substantially larger than obtained from the dc current. On the other hand, the experimental output current trajectory was found to be qualitatively reproduced if the dc current function $i_D^{\rm DC}(\mathbf{u})$ was rescaled by a factor $k_{\rm LFD}$. The optimum $k_{\rm LFD}$ varies with the input power, load, and operation bias. For the considered 5-Ω load agreement of the output power was achieved at SS levels by setting $k_{\rm LFD} = 0.72$. In order to study the effect of the different LFD approaches on power sweep data, we will discuss four models under the assumption that $k^{\rm LFD}$ is a constant. None of these models are intended to give a global description of the LFD phenomena.

The first model disregards LFD. The second model (model Ro) is a simple one-mode Root model [see (67)–(69)] with $\theta_{Ro}^{\rm LFDC}(\mathbf{u}) = (1 - k_{\rm LFD}) i_D^{\rm DC}(\mathbf{u})$ as the equilibrium function. This LFD implementation predicts a uniform reduction of the drain current when the LS excitation is changed from equilibrium (dc) to frozen state (HF). A third model is obtained from the second by a specific nonlinear state transformation (model RoM) for which a change in LS output current is expected according to (84). The fourth model (model VLag) is a two-mode LFD model according to (79)–(81). The second row of the output matrix has been intentionally chosen to equal the gradient of the equilibrium function of model Ro. This way it is accomplished that the models Ro, RoM, and Vlag have the same global SS signature and dc characteristics. However, the current response on a voltage pulse from $(0, 0)$ to $(u_{\rm GS}, u_{\rm DS})$ will be quite different for the four model situations. While the models Ro and RoM lead to a uniform current decrease, the voltage lag model introduces bead-shaped structures in the output characteristics. All models and modes have the same delay time $\tau_{\rm LF} = 1\ \mu$s.

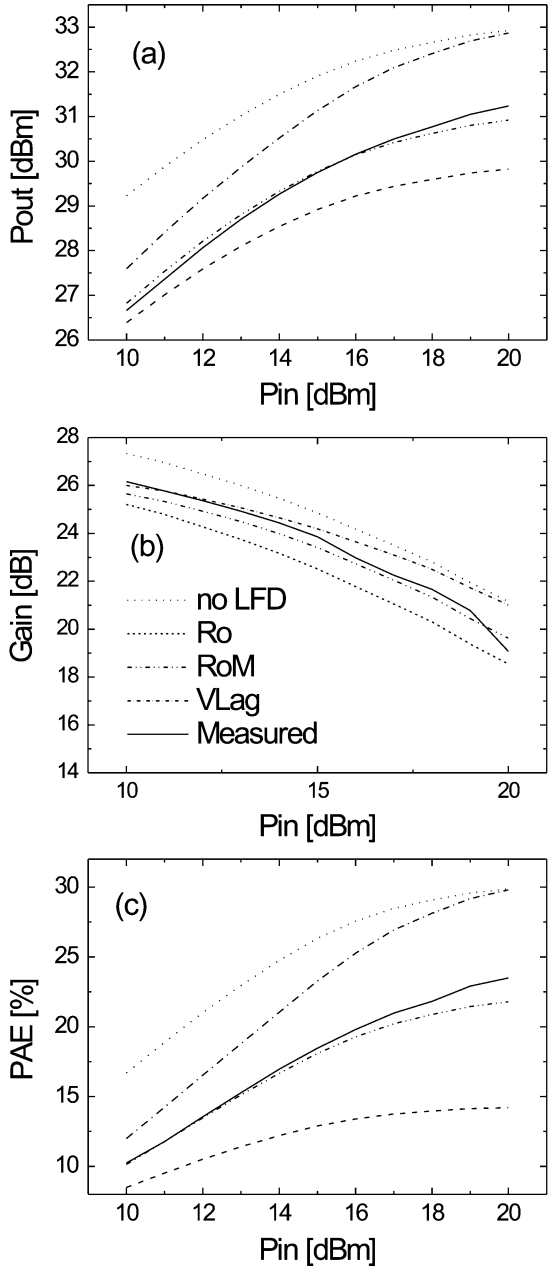

Fig. 2. Power-sweep characteristics for a 8 × 60 GaN HEMT in class AB operation in comparison with predictions from four different LFD models. (a) Output power. (b) Gain. (c) PAE versus input power.

Fig. 2 shows a comparison of the experimental power-sweep characteristics and the model predictions. For very low input power (<1 dBm) output power, gain, and power-added efficiency (PAE) coincide by construction for the models Ro, RoM, and VLag, whereas gain and output power is overestimated if LFD is neglected. As compression starts, the models differ appreciably. While the Root model (in this specific version) underestimates output power and PAE, the VLag model gradually approaches the too optimistic predictions under LFD neglect. For

the model RoM, there is a good correspondence of predicted and measured output power and PAE. This is not surprising since the specific state transform $h(q) = q + 3 \cdot q^{0.7}$ (used to create RoM from Ro) was found by trial and error with the goal to reproduce the compression of the output power without any distortion of the SS signature. This example shows that higher order terms (5) and (10) in the state variables are normally important, but can be possibly compensated for by an appropriate choice of the state representation.

VII. Conclusion

In this paper, we have presented a general and consistent state-variable approach for LS modeling of transistors, which facilitates the treatment of nonlinearity and memory effects. As shown in Section VI, a complete S-parameter data set does not suffice to retrieve all possible output variations and off-equilibrium state configurations accessible under LS excitation; however, it allows for the construction of a state-linear LS model consisting of a relaxation matrix, an output matrix, an equilibrium state function, and an equilibrium output function.

The key entities for model construction are the mode matrices. They satisfy factorization relations with factors, which yield trial input and output matrices. Bias-dependent similarity transformations are employed to obtain appropriate input matrices, which satisfy integrability conditions and provide the equilibrium state functions. In summary, a complete S-parameter data set gives insight into the dimension and the relaxation times of the state space and devises state functions in a state-linearized limit.

From an initial model representation, a large pool of models, which conform with a given SS signature, can be generated by SSE state transforms. An LS database is necessary to prepare from this pool a state-linear or an RSL model or to construct higher order state terms of the state functions.

LFD has been described consistently by states relaxing at LFs. Single- and double-mode approaches have been presented for the description of LFD phenomena and are compared with experimental power-sweep data for a GaN transistor.

References

[1] C. M. Snowden, "Nonlinear modelling of power FETs and HBTs," *Int. J. Microw. Millimeter-Wave Comput.-Aided Design*, vol. 6, pp. 219–234, Jul. 1996.

[2] W. Batty, C. E. Christoffersen, A. J. Pank, S. Davi, C. M. Snowden, and M. B. Steer, "Electro-thermal CAD of power devices and circuits with fully physical time-dependent compact thermal modelling of complex nonlinear 3-D systems," *IEEE Trans. Compon. Packag. Technol.*, vol. 30, no. 3, pp. 566–590, Sep. 2001.

[3] D. Schreurs, J. Verspecht, E. Vandamme, N. Vellas, C. Gaquiere, M. Germain, and G. Borghs, "ANN model for AlGaN/GaN HEMTs constructed from near-optimal-load large-signal measurements," in *IEEE MTT-S Int. Microw. Symp. Dig.*, Jun. 2003, pp. 447–450.

[4] J. Xu, M. C. E. Yagoub, R. Ding, and Q. J. Zhang, "Neural based dynamic modeling of nonlinear microwave circuits," in *IEEE MTT-S Int. Microw. Symp. Dig.*, Jun. 2002, pp. 1101–1104.

[5] A. Alabadelah, T. Fernandez, A. Mediavilla, B. Nauwelaers, A. Santarelli, D. Schreurs, A. Tazon, and P. A. Traverso, "Nonlinear models of microwave power devices and circuits," in *Proc. 12th GaAs Symp.*, Oct. 2004, pp. 191–193.

[6] M. Iwamoto, D. E. Root, and J. Wood, "Device modelling for III–V semiconductors," in *IEEE CSIC Dig.*, 2004, pp. 279–282.

[7] T. Glad and L. Ljung, *Control Theory: Multivariable and Nonlinear Methods*. New York: Taylor & Francis, 2000.

[8] P. Jansen and D. Schreurs, "Consistent small-signal and large signal extraction techniques for heterojunction FET's," *IEEE Trans. Microw. Theory Tech.*, vol. 43, no. 1, pp. 87–93, Jan. 1995.

[9] A. Werthof, F. van Raay, and G. Kompa, "Direct nonlinear power MESFET parameter extraction and consistent modelling," in *IEEE MTT-S Int. Microw. Symp. Dig.*, Jun. 1993, vol. 4, pp. 645–648.

[10] M. C. Foisy, P. E. Jeroma, and H. H. Martin, "Large-signal relaxation time model for HEMTs and MESFETs," in *IEEE MTT-S Int. Microw. Symp. Dig.*, Jun. 1992, pp. 251–254.

[11] I. Schmale and G. Kompa, "A symmetric non quasi-static large-signal FET model with a truly consistent analytic determination from DC- and S-parameter data," in *Proc. 29th Eur. Mircrow. Conf.*, Munich, Germany, Oct. 1999, vol. 1, pp. 258–261.

[12] R. Anholt, *Electrical and Thermal Characterization of MESFETs, HEMTs and HBTs*. Boston, MA: Artech House, 1995.

[13] S. C. F. Lam, P. C. Canfield, and D. J. Allstot, "Modeling of frequency and temperature effects in GaAs MESFETs," *IEEE J. Solid-State Circuits*, vol. 25, no. 2, pp. 299–306, Feb. 1990.

[14] S. C. Binari, P. B. Klein, and T. E. Kazior, "Trapping effects in GaN and SiC microwave FETs," *Proc. IEEE*, vol. 90, no. 6, pp. 1048–1058, Jun. 2002.

[15] A. E. Parker and J. G. Rathmell, "Bias and frequency dependence of FET characteristics," *IEEE Trans. Microw. Theory Tech.*, vol. 51, no. 2, pp. 588–592, Feb. 2003.

[16] E. S. Kuh and R. A. Rohrer, "The state-variable approach to network analysis," *Proc. IEEE*, vol. 53, no. 7, pp. 672–685, Jul. 1965.

[17] D. E. Root, J. Wood, N. Tufillaro, D. Schreurs, and A. Pekker, "Systematic behavioral modeling of nonlinear microwave/RF circuits in the time domain using techniques from nonlinear dynamical systems," in *Proc. IEEE Int. Behavioral Modeling and Simulation Workshop*, Oct. 2002, pp. 71–74.

[18] H. K. Khalil, *Nonlinear Systems*. New York: Macmillan, 1992.

[19] A. Stelzer, R. Neumayer, F. Haslinger, and R. Weigel, "On the synthesis of equivalent circuit models for multiports characterized by frequency-dependent parameters," in *IEEE MTT-S Int. Microw. Symp. Dig.*, Jun. 2002, vol. 43, pp. 721–724.

[20] D. E. Root, "Measurement based active device modelling for circuit simulation," in *23rd Eur. Adv. Microw. Microwave Conf., Devices, Characterization, Modeling Workshop*, 1993, pp. 191–193.

[21] P. A. Traverso, M. Pagani, F. Palomba, F. Scappaviva, G. Vannini, F. Filicori, A. Raffo, and A. Santarelli, "Improvement of PHEMT intermodulation prediction through the accurate modelling of low-frequency dispersion effects," in *IEEE MTT-S Int. Microw. Symp. Dig.*, Jun. 2005, pp. 465–468.

Matthias Seelmann-Eggebert received the Diploma degree and Ph.D. degree in physics from the University of Tübingen, Tübingen, Germany, in 1980 and 1986, respectively.

From 1980 to 1996, he was involved with research and development related to infrared detectors based on HgCdTe and developed electrochemical and surface physical methods for the characterization of compound semiconductor surfaces. From 1990 to 1991, he was a Visiting Scientist with Stanford University. From 1997 to 2000, he was engaged in the growth of chemical vapor deposition (CVD) diamond. Since 2001 he has been a member of the Department of High-Frequency Electronics, Fraunhofer Institute of Applied Solid State Physics (IAF), Freiburg, Germany, where he is concerned with the preparation and development of simulation models for active and passive III–V devices.

Thomas Merkle received the Dipl.-Ing. Degree in electrical engineering from the University of Stuttgart, Stuttgart, Germany, in 1999. His doctoral thesis concerned the investigation of intermodulation distortion in HEMTs, which has been submitted to the University of Ilmenau.

Upon the completion of the M.Sc. degree, he joined the Fraunhofer Institute of Applied Solid State Physics (IAF), Freiburg, Germany, where he was involved with the field of nonlinear characterization and modeling of GaAs and GaN HEMTs, as well as the design of monolithic microwave integrated circuits (MMICs) from 30 to 110 GHz. Since 2005, he has been with the CSIRO ICT Centre, Epping, N.S.W., Australia, where he is involved with the design of active integrated antennas from 60 to 100 GHz. His general research interests comprise devices and systems with wanted and unwanted nonlinear behavior at HFs, especially problems in model identification, parameter extraction, and design methods.

Friedbert van Raay received the M.Sc. degree in electrical engineering from the Technical University of Aachen, Aachen, Germany, in 1984, and the Ph.D. degree from the University of Kassel, Kassel, Germany, in 1990.

From 1992 to 1995, he was with SICAN GmbH, Hannover, Germany, where he was involved with RF system development and measurement techniques. In 1995, he returned to the University of Kassel, as a Senior Engineer, where he supervised the Microwave Group, Institute of High Frequency Engineering. In November 2001, he joined the Fraunhofer Institute of Applied Solid-State Physics (IAF), Freiburg, Germany, as a Supervisor of the Device Modeling Group. His current research interests are development and characterization of high-speed digital and high-power millimeter-wave GaAs and GaN devices and circuits.

Rüdiger Quay (M'01) was born in Cologne, Germany, in 1971. He received the Diplom degree in physics from Rheinisch-Westfälische Technische Hochschule (RWTH) Aachen, Aachen, Germany, in 1997, and the the Doctoral degree in technical sciences (with honors) from the Technische Universität Wien, Vienna, Austria, in 2001.

He currently is a Senior Research Engineer with the Fraunhofer Institute of Applied Solid-State Physics (IAF), Freiburg, Germany. He has authored or coauthored over 50 refereed publications. His scientific interests include RF semiconductor device and MMIC development, heterostructure device modeling and simulation, advanced measurement techniques, and circuit and reliability issues.

Michael Schlechtweg received the Dipl.-Ing. degree in electrical engineering from the Technical University Darmstadt, Darmstadt, Germany, in 1982, and the Dr.-Ing. degree from the University of Kassel, Kassel, Germany, in 1989.

Since 1989, he has been with the Fraunhofer Institute for Applied Solid-State Physics (IAF), Freiburg, Germany, where he was initially involved with the design and characterization of microwave and millimeter-wave integrated circuits and with nonlinear characterization and modeling of active RF devices. Since 1996, he has been Head of the High-Frequency Devices and Circuits Department, where he has focused on the design and the characterization of devices and integrated circuits based on III–V compound semiconductors (GaAs, InP, and GaN) for HF applications. He has authored or coauthored over 150 scientific publications. He holds two patents.

Dr. Schlechtweg was the recipient of the 1993 Fraunhofer Prize and the 1998 European Microwave Prize.